Perceptually Fractural Pixel Values in Rendering High Dynamic Range Images

Yongdong Wu, Bo Qiu

Institute for Infocomm Research, Singapore

ABSTRACT

High Dynamic Range (HDR) images capture the full range of luminance present in real world scenes, and unlike Low Dynamic Range (LDR) images, can simultaneously contain detailed information in the deepest of shadows and the brightest of light sources. In order to render HDR image on LDR displayers, it is often necessary to create LDR depictions of HDR images at the cost of contrast information loss. To reduce the loss, this paper enables to render HDRI (High Dynamic Range Image) with multiple low-bit images periodically. From the viewpoint of a human, the pixel value is fractural. It does not adjust the tones but can reconstruct HDR images.

1. INTRODUCTION

A High Dynamic Range (HDR) image is able to accurately represent the wide range of intensity levels found in real scenes, e.g., sunlight at noon may be as much as 100 million times brighter than starlight.[1] Because their dynamic ranges are broad enough to represent the true range of luminosity in a scene, HDR images capture details that are perceived by the human visual system (HVS). There are 4 ways to obtain HDR images: (1) *Multiple exposure*: It takes a plurality of images the same scene many times with a wide range of exposure settings at different exposure levels, applies neighborhood processing to each of the images, and then combines the components into one HDR image[2–6] , e.g., the "`merge to HDR`" feature of Photoshop CS2; (2) *Computer graphics*: With the digital model of real scene in terms of geometry, lighting, and materials, computer engineers create HDR images allowed for more realistic renditions because the units used were based on actual physical units; (3) *Reverse Tone Mapping*[7]: It boosts the dynamic range of legacy video and photographs for viewing on high dynamic range displays; (4) *HDR camera*[8]: Modern digital cameras can produce an image with a single exposure of a sensor that has a native high dynamic range, e.g., Nikon D3 can output 14bits/channel images.

All the HDR images, real or synthetic, may have luminance spanning 14 orders of magnitude, and are necessary to display images on advanced and expensive HDR display devices, capable of showing contrast of 50,000:1. However, the standard output/viewing devices such as computer monitors have merely the contrast of 700:1, 8-bit images with values between 0 and 255, or a useful dynamic range of around 2 orders of magnitude. The range, while being larger than 2 orders of magnitude, lies partially in the dark end, human vision has trouble discerning very small differences under normal viewing circumstances regardless the human visual system is able to detect 4 or 5 orders of magnitude simultaneously, and can adapt to a range of around 10 orders of magnitude over time.[1]

To render HDR images on devices such as computer monitors (CRTs, LCDs) and printers with a limited dynamic range, various methods have been developed. As the first and most developed research area in HDR image processing, tone mapping compresses the wide dynamic range to a narrower range for display and aesthetic purposes thus creating an LDR depiction of an HDR image. For a majority of existing tone mapping operators this is achieved through the reduction of physical contrast in LDR (Low Dynamic Range) images, each introduces a degree of distortion into the resulting LDR tone mapped image. As indicated in,[9] two major contrast distortions resulting from tone mapping: (1) The contrast ratio between lightest and darkest areas of the HDR is modified in the LDR, (2) the high frequency contrasts (textures and contours) of the HDR image become less prominent, disappear, or become exaggerated in the LDR. In reality, perceived image contrast is not only a function of the dynamic range of the tone mapped image, but also depends significantly on other image attributes such as lightness, hue, chroma, and sharpness.[10] All successful tone mapping operators balance the tradeoff between

Send correspondence to Yongdong Wu: wydong@i2r.a-star.edu.sg, www.i2r.a-star.edu.sg/icsd/staff/yongdong/

Visual Communications and Image Processing 2010, edited by Pascal Frossard, Houqiang Li, Feng Wu, Bernd Girod, Shipeng Li, Guo Wei, Proc. of SPIE Vol. 7744, 77442X · © 2010 SPIE · CCC code: 0277-786X/10/$18 · doi: 10.1117/12.863019

loyal reproduction of the luminance range and preservation of details. As concluded by evaluations of tone mapping operators,[12,13] it is difficult for one tone mapping operator to be well-suited to all types of images.

This paper enables to render HDRI (High Dynamic Range Image) with multiple low-bit images periodically. From the viewpoint of a human, the pixel value is fractural. It does not adjust the tones but can reconstruct.

The rest of the paper are organized as follows. Section 2 presents our fractural pixel scheme. The related work are introduced in Section 3. The concluding remarks are drawn in Section 4.

2. FRACTURAL PIXEL VALUE

The human retina holds two types of photoreceptor cells. Cones sense color and respond well in dim to bright light (0.1 to $10^{+8} cd/m^2$), and rods respond best between darkness and moderate light (10^{-6} to $10 cd/m^2$), but are blinded by saturation above $100 cd/m^2$.[14]

According to papers,[15,16] most retinal cells vary their response only within a range of intensities that is very narrow if compared against the entire range of vision. Adaptation processes dynamically adjust these narrow response functions to conform better to the available light. Time adaptation is an important characters of human eyes. Time-dependent schemes[15,16] map the tone in accordance with the time adaptation model. Exponential decay functions are often used to model temporal processing of the visual system.[17–21]

2.1. Problem definition

With regard to Fig.1, after an imaging system acquires a scene, an engineers synthesizes an image **I** with n_0 bits/channel, the image will be rendered on a display of m_0 bits/channel where $n_0 > m_0$. Thus, the monitor is not able to directly render the image without distortion. To match the image resolution with the display resolution, the present scheme attempts to transfer the integer pixel values into perceptually fractural pixel values so as to provide visual appearance of high fidelity.

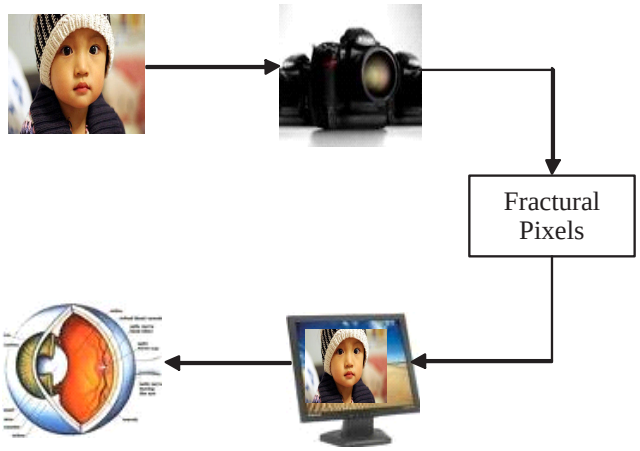

Figure 1. Visual system structure.

More specifically, for any pixel with value p (e.g., Red pixel value), $p = q \times m + r$ where $m = c2^{m_0}$ for some integer c, $0 \leq r < m$, the present scheme aims to render pixel value as

$$\tilde{p} = \frac{p}{m} = q + \frac{r}{m} \tag{1}$$

perceptually instead of q only, and hence increase the visual fidelity.

As few legacy displays can render fractural pixel $\tilde{P}$ in Eq.(1) directly, we must perform some transformations which meet the following criterions:

(1) Contrast ratio remains as close as original. Large, abrupt changes in scene intensities can cause dramatic compression of visual responses, followed by a gradual recovery of normal vision. Asymmetric mechanisms govern these time-dependent adjustments, and offer adaptation to increased light that is much more rapid than adjustment to darkness;

(2) Average value is consistent with the original;

(3) Dynamic property is optimized, i.e., minimize the distortion between the model and the implementation.

2.2. Perceptually fractural pixel value

For each pixel, its value will be sent to the display memory periodically. Hence, if any pixel is always output as $q+1$, the pixel will be brighter than the realistic one, on the contrary, if any pixel is always output as q, it will be darker than the original one if $r \neq 0$. Therefore, it is enough to periodically output the pixel sequence $\{q, q+1\}^m$ in order to render "pixel" $\tilde{p}$ in Eq.(1) such that the real visual appearance is true. That is to say, as shown in Fig.2, we output pixel value q at time t_0 and pixel value $q+1$ at time t_1 such that the perceptual pixel $\tilde{p} = q + \frac{r}{m} \in [q, q+1)$.

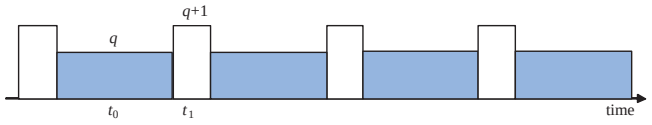

Figure 2. Output pixel value sequence for fractural pixel $\tilde{p} = q + 1/4$.

Albeit the above fractural pixel principle is easy to understand, we should estimate the fidelity of fractural pixel, and how to generate the pixel sequence. Denote the refreshing period is T, and the period is divided into m pieces of time interval τ, i.e., $T = m\tau$ for some integer m, where τ is the refreshing cycle of the display, e.g., τ=10ms for 100HZ displayer.

Lemma 1: A fractural pixel with value $1/m$ can be approximated with a pixel sequence which includes one pixel with value 1 and $(m-1)$ pixels with value 0.
Proof: The human visual system can be approximated as an exponential decay function, *i.e.*,

$$G(s) = \frac{\sigma}{s+\sigma},$$

where the nominator may be other value. Assume that there is an ideal display which can render fractural pixel. For an input signal with value $1/m = \tau/T$ and a sufficiently large time $\theta = kT + \theta_0$, $0 \leq \theta_0 < T$, the human visual appearance is stable, hence its ideal expected average within a period T is

$$\mu_1 = \int_{\theta}^{\theta+T} \mathcal{L}^{-1}(\tau/T(1-e^{-\sigma t}))dt = \tau - \frac{e^{-\sigma\theta}(1-e^{-\sigma T})}{\sigma} \approx \tau \tag{2}$$

where $\mathcal{L}^{-1}(\cdot)$ is the inverse Laplace transform. On the other hand, denote the pixel sequence as a periodical pulse signal $x(t)$ of value 1, width τ and period T, its Laplace transform is

$$X(s) = \mathcal{L}(x(t)) = \frac{1-e^{-\tau s}}{s(1-e^{-Ts})},$$

where $\mathcal{L}(\cdot)$ is the Laplace transform. Thus, for a simulation fractural system, the visual response is

$$Y_1(s) = G(s)X(s) = \frac{\sigma}{s+\sigma} \times \frac{1-e^{-\tau s}}{s(1-e^{-Ts})},$$

correspondingly, the time domain is

$$\begin{aligned} y_1(t) &= \mathcal{L}^{-1}(Y_1(s)) \qquad (3) \\ &= \begin{cases} g_1(t) + (1 - e^{-\sigma(t-kT)}) & t \in [kT, kT+\tau] \\ g_1(t) + e^{-\sigma(t-kT)}(e^{\tau\sigma} - 1) & otherwise \end{cases} \\ g_1(t) &= (e^{\sigma\tau} - 1)\sum_{i=0}^{k-1} e^{-\sigma(t-iT)} = (e^{\sigma\tau} - 1) \times \frac{e^{-\sigma t}(1 - e^{\sigma kT})}{e^{\sigma T} - 1} \\ &= \frac{e^{\sigma\tau} - 1}{e^{\sigma T} - 1} \times e^{-\sigma t}(e^{\sigma kT} - 1) \qquad (4) \end{aligned}$$

where $g_1(t)$ in Eq.(4) is the contribution of previous input for sufficient large t. The total response amplitude (energy) within any interval $(\theta, \theta + T)$ to the simulate pixel sequence is

$$\begin{aligned} \tilde{\mu}_1 &= \int_\theta^{\theta+T} y_1(t)dt \\ &= \int_\theta^{\theta+T} g_1(t)dt + \int_{kT}^{kT+\tau} (1 - e^{-(t-kT)\sigma})dt + \int_{kT+\tau}^{kT+T} \frac{e^{\tau\sigma} - 1}{e^{\sigma(t-kT)}}dt \\ &= \frac{e^{\sigma\tau} - 1}{e^{\sigma T} - 1} \times \frac{e^{-\sigma\theta} - e^{-\sigma(\theta+T)}}{\sigma}(e^{\sigma kT} - 1) + (\tau + \frac{e^{-\tau\sigma} - 1}{\sigma}) - (e^{\tau\sigma} - 1)\frac{e^{-\sigma(\theta_0+T)} - e^{-\tau\sigma}}{\sigma} \\ &= (e^{\sigma\tau} - 1) \times \frac{e^{-\sigma(\theta+T)}}{\sigma}(e^{\sigma kT} - 1) + (\tau + \frac{e^{-\tau\sigma} - 1}{\sigma}) + (e^{\tau\sigma} - 1)\frac{e^{-\tau\sigma} - e^{-\sigma(\theta_0+T)}}{\sigma} \\ &= -(e^{\sigma\tau} - 1) \times \frac{e^{-\sigma(\theta+T)}}{\sigma} + (\tau + \frac{e^{-\tau\sigma} - 1}{\sigma}) + (e^{\tau\sigma} - 1)\frac{e^{-\tau\sigma}}{\sigma} \\ &= \tau - \frac{e^{-\sigma(\theta+T)}(e^{\sigma\tau} - 1)}{\sigma} \approx \tau \qquad (5) \end{aligned}$$

Therefore, the visual appearance $\tilde{\mu}_1 = \mu_1$.

Proposition 1: For large time t, $y_1(t)$ has the same period T as the input function $f_1(t)$.
Proof:
With reference to Eq.(4),

$$\begin{aligned} g_1(t+T) &= \frac{e^{\sigma\tau} - 1}{e^{\sigma T} - 1} \times e^{-\sigma(t+T)}(e^{\sigma kT} - 1) \\ &\approx \frac{e^{\sigma\tau} - 1}{e^{\sigma T} - 1} \times e^{-\sigma t}(e^{\sigma kT} - 1) = g_1(t) \end{aligned}$$

$$\begin{aligned} y_1(t+T) &= \begin{cases} g_1(t+T) + (1 - e^{-\sigma z}) & z \in [0, \tau] \\ g_1(t+T) + e^{-\sigma z}(e^{\tau\sigma} - 1) & otherwise \end{cases} \\ &= y_1(t) \end{aligned}$$

where $z = t - KT$.

Lemma 2 A fractural pixel with value r/m can be approximated with a pixel sequence which includes r pixels with value 1 and $(m - r)$ pixels with value 0.
Proof:
For an input signal with value $r/m = r\tau/T$ to an ideal display, after a sufficiently long time θ, the human visual response is stable, hence the average within period T is

$$\mu_2 = \int_\theta^{\theta+T} r\tau/T dt = r\mu_1 \approx r\tau \qquad (6)$$

On the other hand, the simulated image sequence is a signal function

$$f_2(t) = a_0 x(t) + a_1 x(t-\tau) + \ldots + a_{m-1} x(t-(m-1)\tau),$$

where $a_j \in \{0, 1\}$, and $a_0 + a_1 + \cdots + a_{m-1} = r$. Therefore,

$$F_2(s) = \mathcal{L}(f_2(t)) = \sum_{j=0}^{m-1} a_j e^{-j\tau s} X(s).$$

Thus, the visual appearance is

$$Y_2(s) = F_2(s)G(s) = \sum_{j=0}^{m-1} a_j e^{-j\tau s} G(s)X(s)$$

correspondingly, the time domain is

$$y_2(t) \quad = \quad \mathcal{L}^{-1}(Y_2(s)) = \sum_{j=0}^{m-1} a_j \mathcal{L}^{-1}(e^{-j\tau s} G(s)X(s)) = \sum_{j=0}^{m-1} a_j y_1(t-j\tau) \tag{7}$$

After a sufficiently large time θ, the time domain average within any interval $(\theta, \theta+T)$ is

$$\begin{aligned} \tilde{\mu}_2 &= \int_\theta^{\theta+T} y_2(t)dt = \int_\theta^{\theta+T} \sum_{j=0}^{m-1} a_j y_1(t-j\tau)dt \\ &= \sum_{j=0}^{m-1} a_j \int_\theta^{\theta+T} y_1(t-j\tau)dt = \sum_{j=0}^{m-1} a_j \int_{\theta-j\tau}^{\theta+T-j\tau} y_1(t)dt = \sum_{j=0}^{m-1} a_j \tilde{\mu}_1 \\ &= r\tilde{\mu}_1 \approx r\tau \end{aligned} \tag{8}$$

As $\tilde{\mu}_2 = \mu_2$, Lemma 2 holds.

Proposition 2: For large time t, $y_2(t)$ has the same period T as the input function $f_2(t)$.
Proof:
With reference to Eq.(7) and proposal 1, for large t,

$$y_2(t+T) \quad = \quad \sum_{j=0}^{m-1} a_j y_1(t+T-j\tau) = \sum_{j=0}^{m-1} a_j y_1(t-j\tau) = y_2(t)$$

Proposition 3 Given $u = m/r$ is a integer and If there exist a segmentation such that $a_{iu} + a_{iu+1} + \cdots + a_{iu+u-1} = r/u$ for all $i = 0, \ldots, r-1$, $y_2(t)$ can be regarded as a cycle function with period $u\tau$ for large time.
Proof:
$a_{iu} + a_{iu+1} + \cdots + a_{iu+u-1} = r/u$ for all $i = 0, \ldots, r-1$, hence

$$f_2'(t) = a_0 x(t) + a_1 x(t-\tau) + \cdots + a_{u-1} x(t-u\tau-\tau)$$

is a period function which is the same as the input $f_2(t)$ except the representation. According to proposition 2, function $y_2(t)$ can be approximated as a period function with the same period as the function $f_2'(x)$ for large t.

Lemma 3 A fractural pixel with value $\tilde{p} = q + r/m$ can be approximated with a pixel sequence which includes r pixels with value $q+1$ and $(m-r)$ pixels with value q.
Proof:

For an input signal with value $q + r/m = q + r\tau/T$ to an ideal display, after a sufficiently long time, the human visual response is stable, hence the summation amplitude is

$$\mu_3 = \int_{\theta}^{\theta+T} \mathcal{L}((q + r\tau/T)G(s))dt = qT + r\mu_1 \approx qT + r\tau \quad (9)$$

On the other hand, the simulated image sequence is a signal function

$$f_3(t) = q + a_0x(t) + a_1x(t-\tau) + \ldots + a_{m-1}x(t-(m-1)\tau) = q + f_2(t)$$

where $a_k \in \{0, 1\}$, and $a_0 + a_1 + \cdots + a_{m-1} = r$. Therefore,

$$F_3(s) = L(f_3(t)) = L(q + f_2(t)) = q + F_2(s).$$

Thus, the visual appearance is

$$Y_3(s) = F_3(s)G(s) = qG(s) + F_2(s)$$

or corresponding

$$y_3(t) = \mathcal{L}^{-1}(Y_3(s)) = \mathcal{L}^{-1}(qG(s) + Y_2(s)) = q(1 - e^{-\sigma t}) + Y_2(t) \quad (10)$$

After a sufficiently large time θ, the average response with any interval $(\theta, \theta + T)$ is

$$\begin{aligned} \tilde{\mu}_3 &= \int_{\theta}^{\theta+T} y_3(t)dt \\ &= qT - qe^{-\sigma\theta}(1 - e^{-\sigma T})/\sigma + \tilde{\mu}_2 \\ &\approx qT + r\tau \end{aligned} \quad (11)$$

As $\tilde{\mu}_3 = \mu_3$, Lemma 3 holds.

Proposition 4 Given $u = m/r$ is a integer and If there exist a segmentation such that $a_{iu}+a_{iu+1}+\cdots+a_{iu+u-1} = r/u$ for all $i = 0, \ldots, r-1$, $y_3(t)$ can be regarded as a cycle function with period $u\tau$ for large time.
Proof:
$a_{iu} + a_{iu+1} + \cdots + a_{iu+u-1} = r/u$ for all $i = 0, \ldots, r-1$, hence

$$f_3'(t) = a_0x(t) + a_1x(t-\tau) + \cdots + a_{u-1}x(t-u\tau-\tau)$$

is a period function which is the same as the input $f_3(t)$ except the representation. For large t

$$y_1(t - u\tau) = y_1(t).$$

Therefore, for large t, according to Eq.(10),

$$y_3(T+t) = q(1 - e^{-\sigma(T+t)}) + y_2(T+t) = q(1 - e^{-\sigma(T+t)}) + y_2(t) = y_3(t)$$

Although Lemma 3 ensures that the average visual appearance is close to the original one, the variance of the visual appearance will depend on the sequence $\{a_k\}$. We attempt to select $\{a_k\}$ so as to minimize variance. In the following, $a_j = a_{j \mod m}$ if $j > m-1$.

Lemma 4 The segmentation in lemma 4 is of minimal variance.
Proof:

$$\delta = \int_{\theta}^{\theta+T} (y_3(t) - \mu_3)^2 dt = \sum_{i=0}^{r} \int_{\theta+i\tau}^{\theta+(i+1)\tau} (y_3(t) - \mu_3)^2 dt \leq (\int_{\theta}^{\theta+T} (y_3(t) - \mu_3)dt)^2 \quad (12)$$

where "=" holds if and if $\int_{\theta+i\tau}^{\theta+(i+1)\tau}(y_3(t) - \mu_3)^2 dt$ is constant for all $i = 0, \ldots, r-1$. Based on Lemma 4, we can select the period of input function as u.

3. RELATED WORK

[23] Nine algorithms were implemented to overcome the problem associated with rendering high-dynamic-range scientific imagery to low dynamic-range display devices. The algorithms were evaluated using two paired-comparison psychophysical experiments judging preference and "scientific usefulness". Reinhard et al.[24] addressed some algorithms for HDR rendering on LDR display too. Ledda et al.[25] evaluates their performances.

3.1. Direct Mapping

A naïlve tone mapping method select a "window" of the entire dynamic range, and clips to set minimum and maximum values. However, more recent methods have attempted to compress the dynamic range into one reproducible by the intended display device. The more complex methods tap into research on how the human eye and visual cortex perceive a scene, trying to show the whole dynamic range while retaining realistic color and contrast.

Tumblin and Rushmeier[26] developed a tone mapping operator using models of human perception using a global brightness adaptation, dark and bright regions are clipped. Larson et al.[27] proposed a global tone mapping operator which adjusts the histogram of the scene based on psychophysical models for color, glare, and acuity perception noted by Ferweda et al..[28] Global tone mapping methods.[26,27] are reasonably successful in resolving the tone reproduction problem and avoid visual artifacts such as halos, especially to images whose histogram is bimodal with a large gap between the modes, they tend to lose the local details of the scene.

By contrast, local tone mapping methods such as those presented in[29–36] not only provide a good tone reproduction performance, but also preserve the finer details of the original scene. Such approaches typically mimic the human visual system by computing the local adaptation luminance in the scene. When computing the local adaptation luminance, the size of the local region is a crucial consideration and is generally estimated using some form of local contrast measure.

Fuh et al.[37] convert luminance values associated with pixels into a plurality of luminance values, and utilize a film transfer function for mapping the new luminance values associated with the pixels into a plurality of luminance values to generate the low dynamic range image.

3.2. Device adaptive

Because of the variety of display technologies (LCD, LCoS, PDP, DLP, OLED, e-paper etc.), their applications and viewing conditions, the display devices can differ dramatically in their peak brightness, contrast and black level, it cannot be expected that the same image shown on different devices will produce the desirable appearance. Mantiuk et al.[38] proposed a mapping technique that can adjust image or video content for optimum contrast visibility taking into account ambient illumination and display characteristics. They weighted contrast distortions according to their visibility predicted by the model of the human visual system, and further minimize the distortions given a display model.

3.3. Multi-level separation

In,[39] a synthetic HDR image is decomposed into layers of lighting and surface properties. The light layer, which contains most of the high contrast, is compressed and added back to the surface layers containing details and texture. In this way, high contrast is reduced while preserving the details and texture from the original image.

For a natural HDR image, Xu et al.[40] separated it into detail and profile. Then they uses a global tone mapping function to compress the profile, and then produce a LDR version of the image for display by adding the details to the compressed profile. This method is capable of compressing the dynamic range while retaining the detail in the final image of various HDR images in a short time.

3.4. Multi-scale

Pattanaik et al.[41] proposes a multiscale model for the representation of pattern, luminance and color in the human visual system. Similar to the work of Pattanaik et al., we have the multiscale generalization[42,43] of the Retinex algorithm.[44] In this approach, to avoid the appearance of halos close to strong edges,[43] is necessarily to finely tune the weighting of the different scales.[42] In terms of dynamic range compression, it performs well for moderate dynamic range compression but not for high dynamic range compression.[42]

Continuing with the idea of segregating the image into layers of lighting and details, Tumblin and Turk[35] proposed a multiscale approach to extract a hierarchy of details and boundaries. They started with a sketch of strong features and progressively add small details, and decomposed the image into strong and weak features using a multiscale operator, then, only strong features are compressed.

Based on spatial and statistical information, Li et al.[45] decomposed a HDR image into a base layer and a detailed layer, which represent its smoothed and fine details, respectively. The problem of overall impression preservation is regarded as a global issue in our algorithm. Statistical-based histogram adjustment is employed to deal with the base layer. The reproduction of visual details is regarded as a local issue. The detailed layer obtained using a spatial filter is adaptively enhanced according to the mapping function used for the base layer.

In the subband architecture,[46] a symmetrical analysis-synthesis flter bank is applied local gain control to the subbands. We also show that the technique can be adapted for the related problem of companding, in which an HDR image is converted to an LDR image, and later expanded back to high dynamic range.

3.5. Multiple Images

In contrast with rendering HDR image with a single image with reduced range, multiple images scheme[47] produces a minimal set of images capturing the information all over the high dynamic range data, while at the same time preserving a natural appearance for each one of the images in the set.

Tumblin et al[39] proposed a locally adaptive method, denoted as the foveal display, which is inspired by eye movements. The user selects a point of attention and the algorithm computes an output image with preserved contrast in the foveal region (a region around the selected point). It is important to remark that this approach is dynamic in the sense that a set of images is generated with the aid of user interaction.

[15] derived a new tone reproduction operator that simulates these mechanisms. The operator accepts a stream of scene intensity frames and creates a stream of color display images. All operator components are derived from published quantitative measurements from physiology, psychophysics, color science, and photography. Kept intentionally simple to allow fast computation, the operator is meant for use with real-time walk-through renderings, high dynamic range video cameras, and other interactive applications. The operator is simple, uses global rather than local adaptation models

Kentaro et al.[48] constructed a background image constructed from HDR image information is displayed along with portions of the HDR image corresponding to one or more regions of interest. Furthermore, an intermediate LDR image is determined based on image data corresponding to one or more regions of interest of the HDR image. The intermediate image or a derived image is then displayed.

4. CONCLUSION

The simple and elegant method is very good and with high fidelity to the subjective perception of the scene. Note that since this method tries to preserve the original perception of the scene, details that are hard to see in the original scene will be difficult to see in the output image as well. However, the present scheme requires that the render device can manipulate the image bit planes so as to create the image sequence.

REFERENCES

1. J.A. Ferwerda, "Elements of early vision for computer graphics," IEEE Computer Graphics and Applications, 21(5):22-33, 2001.
2. R. Ginosar, O. Hilsenrath, and Y. Zeevi, "Wide dynamic range camera", US patent 5,144,442, Sept. 01, 1992.
3. Paul Debevec, and Jitendra Malik, "Recovering High Dynamic Range Radiance Maps from Photographs", SIGGRAPH, 1997. http://www.debevec.org/Research/HDR/.
4. Steve Mann, "Compositing Multiple Pictures of the Same Scene", 46th Annual Conference on IS&T, 1993.
5. S. Mann and R. W. Picard, "On Being Undigital With Digital Cameras: Extending Dynamic Range By Combining Differently Exposed Pictures", Annual Conference on IS&T, pp.422-428, 1995.
6. Ming-Chian Sung, Te-Hsun Wang, and Jenn-Jier James Lien, "High Dynamic Range Scene Realization Using Two Complementary Images," ACCV, LNCS 4843, pp.261-270, 2007.
7. Allan G. Rempel, Matthew Trentacoste, Helge Seetzen, and H. David Young, "Ldr2Hdr: On-the-fly Reverse Tone Mapping of Legacy Video and Photographs," ACM Transactions on Graphics, Vol.26, No.3, Article 39, 2007. http://www.cs.ubc.ca/~heidrich/Projects/Ldr2Hdr/
8. S.K. Nayar, and T. Mitsunaga, "High dynamic range imaging: Spatially varying pixel exposures," IEEE CVPR, pp.1472-1479, 2000.
9. Kaleigh Smith, Grzegorz Krawczyk, Karol Myszkowski, and Hans-Peter Seidel, "Beyond Tone Mapping: Enhanced Depiction of Tone Mapped HDR Images," EUROGRAPHICS, 25(3):427-438 (2006).
10. A. Calabria, and M. Fairchild, "Perceived image contrast and observer preference: The effects of lightness, chroma, and sharpness manipulations on contrast perception," J. Imag. Sci.and Tech. 47:479-493, 2003.
11. Feng Xiao, Jeffrey M. DiCarlo, Peter B. Catrysse, and Brian A. Wandell, "High Dynamic Range Imaging of Natural Scenes",
12. A. Yoshida, V. Blanz, K. Myszkowski, and H.-P Seidel, "Perceptual evaluation of tone mapping operators with realworld scenes," SPIE Human Vision and Electronic Imaging X, volume 5666, pp.192-203, 2005.
13. P. Ledda, A. Chalmers, T. Troscianko, and H. Seetzen, "Evaluation of tone mapping operators using a high dynamic range display," ACM Transactions on Graphics 24(3):640-648, 2005.
14. D. C. Hood, and M. A. Finkelstein, "Sensitivity to light. In Boff, K. R., Kaufman, L. R. and Thomas, J. P. (ed.), Handbook of Perception & Human Performance, Chapter 5, New York: Wiley, 1986.
15. Sumanta N. Pattanaik, Jack Tumblin, Hector Yee, Donald P. Greenberg, "Time-dependent visual adaptation for fast realistic image display," ACM SIGGRAPH, pp.47-54, 2000.
16. Patrick Ledda,Luis Paulo Santos, Alan Chalmers, "A local model of eye adaptation for high dynamic range images," ACM Afrigraph, pp.151-160, 2004.
17. E. H. Adelson, "Saturation and adaptation in the rod system," Vision Res., vol.22, pp.1299-1312, 1982.
18. W. S. Geisler, "Effects of bleaching and backgrounds on the flash response of the cone system," Journal of Physiology, vol.312, pp.413-434, 1981.
19. M. M. Hayhoe, N. I. Benimoff, and D. C. Hood, "The time-course of multiplicative and subtractive adaptation process," Vision Research, vol.27, pp.1981-1996, 1987.
20. N. Graham, and D. C. Hood, "Modeling the dynamics of light adaptation: the merging of two traditions," Vision Research, vol.32, pp.1373-1393, 1992.
21. G. Sperling, and M.M. Sondhi, "Model for visual luminance discrimination and flicker detection," Journal of the Optical Society of America, vol.58, pp.1133-1145, 1968.
22. B. H. Crawford, "Change of visual sensitivity with time," Proc. of the Royal Soc., B123, pp.69-89, 1937.
23. Sung Ho Park, Ethan D. Montag,"Evaluating tone mapping algorithms for rendering non-pictorial (scientific) high-dynamic-range images," J. Vis. Commun. Image R., vol.18, pp.415-428, 2007.
24. Erik Reinhard,Timo Kunkel, Yoann Marion, Jonathan Brouillat, Rémi Cozot, Kadi Bouatouch, "Image Display Algorithms for High and Low Dynamic Range Display Devices,".
25. Patrick Ledda, Alan Chalmers, Tom Troscianko, Helge Seetze, "Evaluation of tone mapping operators using a high dynamic range display," ACM Transactions on Graphics, 24(3):640-648, 2005.

26. J. Tumblin, H. Rushmeier, "Tone Reproduction for Computer Generated Images," IEEE CG&A 13(6):42-48 (1993)
27. G.W. Larson, H. Rushmeier, and C. Piatko, "A visibility matching tone reproduction operator for high dynamic range scenes," IEEE Trans. Visual. Comput. Graph., 3(4):291-306, 1997.
28. J. Ferwerda, S. Pattanaik, P. Shirley, and D. Greenberg,"A model of visual adaptation for realistic image synthesis," in SIGGRAPH, pp.249-258, 1996.
29. M. Ashikhmin, "A Tone Mapping Algorithm for High Contrast Images," 13th Eurographics, 145-156 (2002)
30. H. T. Chen, T. L. Liu, and C.S. Fuh, "Tone Reproduction: A Perspective from luminance Driven Perceptual Grouping," IJCV, vol. 65, pp.73-96, 2005.
31. R. Fattal, D. Lischinski, M. Werman, "Gradient Domain High Dynamic Range Compress," ACM SIGGRAPH, pp.249-256, 2002.
32. E. Reinhard, M. Stark, P. Shirley, J. Ferwerda, "Photographic Tone Reproduction for Digital Images," ACM SIGGRAPH, pp.267-276,2002.
33. Jeffrey M. DiCarlo and Brian A. Wandell, "Rendering high dynamic range images," SPIE Electronic Imaging conference, vol.3965, pp.392-401, 2000.
34. F. Durand, and J. Dorsey, "Fast bilateral fltering for the display of high-dynamic-range images," ACM SIGGRAPH, pp.257-266, 2002.
35. J. Tumblin, and G. Turk, "LCIS: A Boundary Hierarchy for Detail-Preserving Contrast Reduction," ACM SIGGRAPH, pp.83-90, 1999.
36. C. Schlick, "Quantization techniques for the visualization of high dynamic range pictures," Eurographics Workshop on Rendering, pp.7-20, 1994.
37. Chiou-Shann Fuh, and Chik-Yau Foo, "Method and an apparatus for transforming a high dynamic range image into a low dynamic range image," US2005117799(A1), 2005-06-02.
38. Rafal Mantiuk, Scott Daly, Louis Kerofsky, "Display Adaptive Tone Mapping,"
39. J. Tumblin, J. Hodgins, and B. Guenter, "Two methods for display of high contrasted images, ACM Trans. Graphics, 18(1):56-94, Jan. 1999.
40. Ruifeng Xu,Sumanta N. Pattanaik, "High Dynamic Range Image Display Using Level Set Framework",
41. S. Pattanaik, J. Ferwerda, M. Fairchild, and D. Greenberg, "A multiscale model of adaptation and spatial vision for realistic image display, ACM SIGGRAPH, pp.287-298, 1998.
42. Z. Rahman, D. Jobson, and G. Woodell, "A multiscale retinex for color rendition and dynamic range compression, SPIE, vol. 2847, 1996.
43. D. Jobson, Z. ur Rahman, and G.Woodell, "Properties and performance of a center/sorround retinex," IEEE Trans. Image Processing, vol.6, pp.451-462, Mar. 1997.
44. E. Land, and J. McCann, "Lightness and retinex theory," J. Opt. Soc. Amer., 63(1):1-11, 1971.
45. Xiaoguang Li, Kin Man Lam, and Lansun Shen, "An adaptive algorithm for the display of high-dynamic range images," J. Vis. Commun. Image R. 18:397-405, 2007.
46. Yuanzhen Li, Lavanya Sharan, and Edward H. Adelson, "Compressing and companding high dynamic range images with subband architectures," ACM Transactions on Graphics 24(3):836-844, 2005.
47. Alvaro Pardo, and Guillermo Sapiro, "Visualization of High Dynamic Range Images," IEEE Trans. on Image Processing, 12(6):639-647, 2003.
48. Toyama Kentaro, "High dynamic range image viewing on low dynamic range displays," US2006158462 (A1), 2006-07-20.